

# Design of adsorption column for reclamation of methyldiethanolamine using homogeneous surface diffusion model

Pravin Kannan\*, Priyabrata Pal, and Fawzi Banat\*

Department of Chemical Engineering, Khalifa University, P.O. Box: 127788, Abu Dhabi, United Arab Emirates

Received: 7 April 2020 / Accepted: 14 September 2020

**Abstract.** A predictive simulation model was applied to design a fixed-bed adsorber for studying the removal of Total Organic Acid (TOA) anions from lean Methyldiethanolamine (MDEA) solution using Calcium Alginate Bentonite (CAB) clay hybrid composite adsorbent. Unlike other conventional techniques typically used for packed bed design, the predictive Homogeneous Surface Diffusion Model (HSDM) does not require any test column breakthrough curves *a priori*. Mass transfer coefficients and isotherm model parameters are provided as input data to HSDM for simulating column breakthrough curves. Various isotherm models were fitted to batch equilibrium data for TOA adsorption on CAB composite adsorbent. Based on Akaike Information Criterion (AIC), Freundlich isotherm was selected and the model parameters were obtained by non-linear regression. Film transfer coefficients and surface diffusivities were determined using appropriate empirical correlations available in the literature. HSDM predictions were first validated using lab-scale column adsorption data generated at lower residence times. The effects of dimensionless numbers (Biot and Stanton) on breakthrough times were investigated using the dimensionless HSDM system and a suitable scale-up regime ( $Bi \sim 1$  and  $St > 10$ ) was established wherein the sensitivity of mass transfer parameters would be minimal. Using similitude rules on key design parameters, a pilot-scale adsorption column was designed and breakthrough curves were generated using the validated HSDM. The appropriateness of the design technique was verified by comparing the estimated breakthrough data and column design parameters with conventional scale-up and kinetic approaches.

## 1 Introduction

Almost all natural gas has  $H_2S$ ,  $CO_2$  or both that needs to be removed before the gas is pumped through transmission pipelines. The sweetening process is carried out using aqueous Methyldiethanolamine (MDEA, 45–50 wt.%) in a regeneration column where heat is applied to strip the acid gas components and recover lean/aqueous MDEA solution (Keewan *et al.*, 2018; Mehassouel *et al.*, 2018; Younas and Banat, 2014). However, contamination of industrial lean MDEA from heat stable salts such as total organic acids (produced by the reaction between aerial oxygen and  $CO_2/H_2S$ ) and heavy metal ions like chromium, lead, etc. (produced from the makeup water or due to the metal corrosion or erosion caused during the continuous running of the plant) always remain a challenge to the gas industry (Cummings *et al.*, 2007; Pal *et al.*, 2015).

The acidic heat stable salts play a vital role in the regeneration column, acting as enhancers for the stripping process. On the other hand, the presence of HSS (Heat

Stable Salts) in a lean amine solution is detrimental to the absorption process intended for amine enrichment (Verma and Verma, 2009; Weiland, 2008). Hence, partial removal of Total Organic Acid (TOA) anions from aqueous amines is crucial for avoiding some operational issues encountered during natural gas sweetening process. Different methods have been used for the removal of Heat Stable Salts (HSS) from amine solvents in natural gas sweetening units. Currently, vacuum distillation, electrodialysis, ion exchange, and adsorption are used for the removal of HSS from lean MDEA solutions. Adsorption is widely used among others and has been in practice for several years. The technique is efficient, easy to operate, and requires low maintenance cost (Edathil *et al.*, 2020). The removal has mainly been facilitated through the development of novel adsorbents, including Calcium Alginate Bentonite (CAB) clay composites that serve to remove TOA and metal ions from lean amine solvents (Pal *et al.*, 2013). The oxidative degradation of MDEA produces high concentrations of organic acid anions that remain as contaminants in the solvent. MDEA contains both amine and hydroxyl groups that adhere strongly to these contaminants, thereby making separation by any available technique largely

\* Corresponding authors: [pravin.kannan@ku.ac.ae](mailto:pravin.kannan@ku.ac.ae);  
[fawzi.banat@ku.ac.ae](mailto:fawzi.banat@ku.ac.ae)

challenging. Calcium alginate biopolymer contains two functional groups, namely carboxyl and hydroxyl groups that serve as adsorption sites and aid in the removal of organic acid anions from a lean MDEA solution. Further, reinforcing bentonite into the alginate matrix increases the mechanical properties, density, and adsorptive efficiency (Edathil *et al.*, 2018; Pal *et al.*, 2019).

However, testing the efficiency of the adsorbent in a broad range of process conditions is sometimes not feasible due to the sensitive nature of MDEA that would otherwise alter the physical properties. For instance, it is a challenging task to generate adsorption equilibrium data as any dilution to lean amine solution would result in significant changes in pH, viscosity and other molecular properties that would significantly affect the stripping tendency of the solvent. Due to these limitations in adsorbent performance testing, reliable simulation capable of accurately modeling the breakthrough behavior under real plant conditions is imperative. Such models could be beneficial for scale-up studies by identifying critical design parameters, interpreting lab-scale test results, and designing full-scale adsorber.

For the design of fixed bed adsorber, many methods have been developed that could be categorized into short-cut or scoping methods and rigorous methods (Crittenden and Thomas, 1998; Patel, 2019). Design of fixed-bed adsorption column by short-cut methods including Mass Transfer Zone Length (MTZL) model, Length of Unused Bed (LUB), Empty Bed Contact Time (EBCT) method, Bed Depth Service Time (BDST) method, Transfer Unit Approach (NTU and HTU) and breakpoint capacity methods requires lab-scale, pilot-scale or plant-scale experimentally determined Breakthrough Curve (BTC) data. On the other hand, rigorous methods are based on complex solutions of the conservation, transport and equilibrium relationships. Under certain assumptions, a simplified analytical solution (equilibrium and reaction rate models) could be obtained for BTC prediction that is, however, limited for specific cases.

Predictive models, on the other hand, consider all the sub-processes of film transfer, intraparticle diffusion, and adsorption kinetics to generate the complete sinusoidal shaped BTC. This is achieved by the development of advanced numerical techniques that aid in solving the complex set of partial differential equations used to describe the column behavior. A brief review of literature indicates that predictive models have been developed and employed for ion exchange and fixed-bed adsorption operations in wastewater/water treatment (Chowdhury *et al.*, 2015; Crittenden *et al.*, 1986a; Hand *et al.*, 1984, 1989; Hudaya and Rachmat, 2019; Srivastava *et al.*, 2008). The most commonly used general rate models are usually considered as complete models since they predict the entire breakthrough curves of the adsorption process (Xu *et al.*, 2013). Among these, the Homogeneous Surface Diffusion Model (HSDM) has been successfully proved and thus, is widely used for predicting the fixed bed adsorber dynamics of many adsorbate/adsorbent systems. Generally, a complete BTC model would constitute the material balance equation, the equilibrium relationship and a set of equations that describe the external and internal mass transfer processes. Since dispersion is negligible in typical adsorption process flow

conditions, mass balance equation based on plug flow type was considered. The superficial velocity was assumed to be constant along the bed as removal of trace TOA components from bulk MDEA solution will pose a negligible effect on material balance. It was also assumed that surface diffusion is the predominant intraparticle mass transfer mechanism and is not a function of local liquid concentration. Many complete BTC models that encompass all three mass transfer processes (film, pore, and surface diffusion) have been reported in the literature (Crittenden *et al.*, 1987). These models differ in the assumptions about the flow processes and mass transfer mechanisms used to describe the column behavior. Homogeneous Surface Diffusion Model (HSDM) has been successfully employed to predict the fixed-bed dynamics for many adsorbate-adsorbent systems reported earlier (Hand *et al.*, 1984). Many simulation packages [FAST, AdDesignS<sup>TM</sup>] that have been developed utilize HSDM (dimension and dimensionless forms), along with a powerful numerical solver for simultaneously solving the complex transport-reaction equations and non-linear adsorption isotherms to predict the breakthrough behavior of the column satisfactorily. Like other predictive models, HSDM requires minimal equilibrium data on isotherms and mass transfer characteristics that could be sourced from literature or through lab-scale experiments.

For the mass-transfer controlled process, column design could be solely based on techniques that employ similitudes in mass transfer characteristics. A frequently employed method for full-scale performance prediction is the Rapid Small-Scale Column Test (RSSCT) that employs scaling relationships of the design and operational parameters between the small-scale and large-scale adsorber. By maintaining perfect similarity and using a relatively smaller adsorbent particle, the RSSCT would exhibit identical breakthrough profiles as the full-scale unit (Crittenden *et al.*, 1991). Few other researchers also accomplished similarity between scales by maintaining the dimensional parameters namely, solute distribution parameter ( $D_g$ ), the surface diffusion modulus ( $Ed = St/Bi$ ), Stanton number ( $St$ ) and Reynolds number ( $Re$ ) (Crittenden *et al.*, 1986b; Hand *et al.*, 1983). Equating the dimensionless parameters of the small-scale and full-scale column, mathematical equations describing the relationships between the critical design parameters were established. However, the derived relationships required varying adsorbent particle diameters between the scales to maintain similitudes. Predictive models are more advantageous when constant particle size needs to be maintained between the scales to minimize any operational and hydraulic problems in full-scale unit. This is particularly true for some adsorbent materials where it is practically impossible to engineer uniform particle size during synthesis. Hence, in the scale-up of fixed-bed adsorption columns, typically particle size and hydraulic loading rate or superficial velocity remain unchanged between the scales. However, it is not feasible to keep the velocity fixed during scale-up due to geometrical design limitations in  $L/D$  ratio of the lab-scale column (Inglezakis and Pouloupoulos, 2006). In fact, when higher velocities were used at larger scales, it offered increased advantages in terms of driving the system to diffusion

control rather than film control. In other words, it resulted in higher breakthrough times as film resistances are minimized, and uniform flow distribution inside the column. Any issues associated with higher velocities, like attrition and fluidization, could be easily resolved by switching to downflow operation in large-scale unit.

Inglezakis and Poulopoulos (2006) have summarized the critical design parameters and the influence it may have on the performance of fixed-bed operations. As it can be seen from Table 1, apart from particle size, contact time is another critical parameter that has a significant effect on breakthrough times. By maintaining similar particle size and contact times, results from lab-scale studies could be directly transferred to plant-scale making the scale-up procedure more simple and precise. However, contact times and the resulting breakthrough times encountered in lab-scale are too small and impractical to be employed in plant-scale operations where higher breakthrough times are desired. Therefore, apart from other similitude rules mentioned in Table 1, particle size and superficial velocity are typically maintained constant in the conventional scale-up techniques.

As it can be seen, the optimum scale and design depends on several key variables associated with the adsorbent characteristics and process variables. It can be challenging to determine the appropriate pilot-scale residence time and loading rates with an experimental method that is based only on column breakthrough studies. Numerous experiments may be required to conclude on the design values, including flow characteristics making the approach costly and time-consuming. Hence, an efficient predictive model in conjunction with dimensionless number(s) that define the mass transfer behavior would be necessary to ensure similitudes during the design process. For example, column adsorption process has been successfully modeled by HSDM and characterized using Bi number by several researchers (Hand *et al.*, 1983; Lee *et al.*, 1983; Smith, 1997; Traegner and Suidan, 1989; Wolborska, 1999). However, in an application towards adsorption of arsenate and other contaminants using granular ferric hydroxide filters, Sperlich *et al.* (2008) concluded that characterization based on Bi number alone was not sufficient to completely characterize the HSDM model. It was suggested to complement Bi with St number in order to predict the BTC satisfactorily and no dimensionless similarities were required. In the current work, a similar approach has been demonstrated to design a pilot-scale fixed-bed adsorption column for TOA adsorption using CAB particles.

Simulation and column design of TOA adsorption from lean MDEA solutions has never been reported in literature till date. The objective of the present work is to utilize HSDM for designing a fixed bed adsorber removing TOA present in lean MDEA solution. A series of lab-scale breakthrough experiments would be conducted at different hydraulic loading rates using different sized columns packed with CAB adsorbent. These experiments would serve to validate the HSDM results and assess the qualitative features of the model in terms of breakthrough curves. The optimum design range would be established based on sensitivity analysis of Bi and St in conjunction with certain

**Table 1.** Critical design parameters reproduced from Inglezakis and Poulopoulos (2006).

Parameter	Comments
$L/U_s$	Critical
$L/d_p$	Minimal effect if it is higher than 150
$L/D$	Minimal effect if it is greater than 5
$D/d_p$	Minimal effect if it is higher than 30 and geometrical similarity can be ignored
$Re_p$	Minimal effect if $L/d_p > 150$
$d_p$	Critical
$E$	Minimal effect if $d_p/D < 0.1$
$U_s$	Minimal effect if solid diffusion is rate-controlling and if the unit operation is in up-flow mode

critical design parameter guidelines available in literature. Finally, the appropriateness of the design technique would be verified by comparing the scale-independent HSDM predictions with conventional scale-up and kinetic approaches. Figure 1 illustrates the overall design methodology employed in this work.

## 2 Method description

### 2.1 Selection of isotherm model

Equilibrium experiments were performed using a batch system to generate TOA-CAB adsorbent isotherm data, and the results have been published in the literature (Edathil *et al.*, 2020). In this study, the batch experimental data were evaluated with the isotherm models of Langmuir, Freundlich, Jovanovic, Two-step Langmuir, Langmuir-Freundlich, Fritz-Schlunder and Li, and the constants were obtained by non-linear regression. A standard procedure in choosing an appropriate model equation is based on the value of regression coefficient ( $R^2$ ). However, regression coefficients and other error functions are prone to error when comparing equations with different degrees of freedom (Dávila-Jiménez *et al.*, 2014). To overcome this problem, Akaike Information Criterion (AIC) was used to rank the isotherm models since it is more sensitive to model deviations and takes into consideration the number of parameters in an equilibrium isotherm model, unlike other error functions. The AIC values for all the models mentioned above were calculated using the following expression:

$$AIC = N \ln \left( \frac{SSE}{N} \right) + 2N_p + \frac{2N_p(N_p + 1)}{N - N_p - 1}, \quad (1)$$

where  $N$  is the number of isotherm data points, SSE is the sum of squared residuals and  $N_p$  is the number of fitted parameters. As can be seen, AIC takes both accuracy and model complexity into account while regression coefficients consider only accuracy as the determining factor. For a given experimental dependent variable response

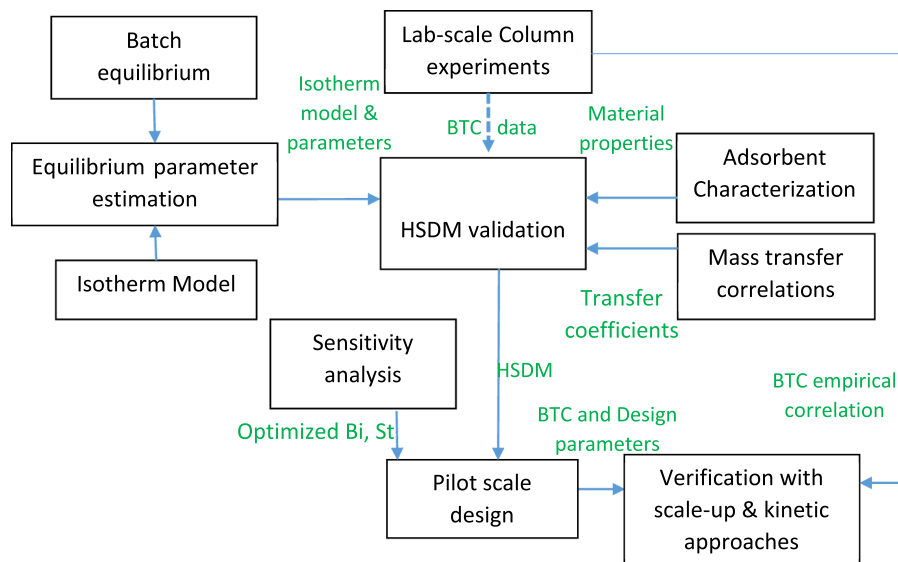


Fig. 1. HSDM based fixed-bed adsorber design technique employed in this study.

(equilibrium solid concentration) on the independent variable (influent concentration), the above-mentioned models with a different number of parameters could be rated based on the values of model AIC's. The particular isotherm model that exhibits the lowest AIC value would best describe the equilibrium between the adsorbent and adsorbate under consideration.

### 2.2 Lab-scale column experiments

Adsorbent material properties of CAB adsorbent including porosity and density were reported in previous works (Edathil *et al.*, 2018). Figure 2 presents a schematic of the fixed-bed adsorption setup used in this work for the removal of TOA from lean MDEA solution. The adsorption system was designed to treat industrial lean MDEA solution and provide clean MDEA (without TOA) at the outlet of the column. The system was designed in such a way that the same column could be utilized for both adsorption and regeneration. Adsorption studies were conducted using different borosilicate glass columns (BUCHI, Switzerland) of varying dimensions ( $d$  (cm)  $\times$   $h$  (cm)):  $1.5 \times 10$ ,  $2.6 \times 10$ ,  $2.6 \times 23$  and  $4.6 \times 23$ ). The column was filled with a known quantity of 2% CAB adsorbent and then lean MDEA solution of known TOA concentration was pumped through the column using a peristaltic pump at the desired flow rate in an up-flow mode. Treated MDEA effluent samples were collected from the outlet of the column at definite time intervals and the concentration of TOA ions in the effluent was measured using a UV-vis spectrophotometer. The operation of the column was stopped once the concentration of TOA ions in effluent samples reached the influent concentration. All adsorption experiments were performed at room temperature and an influent  $pH \sim 10.5$ . For the column dimensions and flow rates considered in this study, the Empty Bed Contact Time (EBCT) varied from 23.5 min to 382 min.

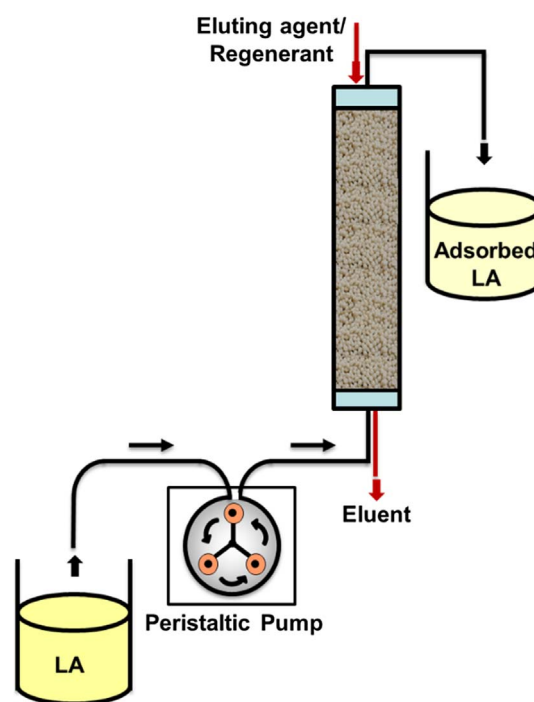


Fig. 2. Schematic diagram representing the fixed-bed column adsorption setup.

### 2.3 BTC predictive model

In this work, a complete Breakthrough Curve (BTC) model considering both adsorption equilibrium and kinetics was used to model the real S-shaped BTCs for TOA adsorption on CAB adsorbents. HSDM is simultaneously represented by two partial differential equations that describe the macroscale liquid phase fluid movement over a bed of adsorbent particles (Eq. (2)) and the unsteady state surface diffusion into the spherical adsorbent particle (Eq. (3)):

**Table 2.** Column parameters used in HSDM validation study.

Parameter	Test 1	Test 2	Test 3	Test 4	Test 5
Height, $L$ (cm)	10	10	23	23	23
Bed diameter, $D$ (cm)	1.5	2.6	4.6	2.6	4.6
Intraparticle porosity, $\varepsilon$	0.85	0.85	0.85	0.85	0.85
Bed porosity, $\varepsilon_b$	0.48	0.46	0.35	0.45	0.36
Particle diameter, $d_p$ (mm)	1	1	1	1	1
Particle density, $\rho_p$ (g/cc)	1.04	1.04	1.04	1.04	1.04
Equivalent bed mass, $M$ (g)	9	29	255	70	255
MDEA flow rate, $Q$ (mL/min)	0.75	0.75	4.3	0.75	1
Empty bed contact time (min)	23.5	71	89	163	382
Superficial velocity, $U_s$ (cm/min)	0.42	0.14	0.26	0.14	0.06
Residence time, $T$ (min)	8.45	25.4	34	58	137
Freundlich coefficient, $K_F$ ((mg/g)(L/mg) <sup><math>n</math></sup> )	0.0015	0.0015	0.0015	0.0015	0.0015
Freundlich exponent, $n$	0.8	0.8	0.8	0.8	0.8
Film mass transfer coefficient, $k_L$ (cm/s)	6.9E-05	4.8E-05	5.3E-05	4.8E-05	5.1E-05
Surface diffusion coefficient, $D_s$ (cm <sup>2</sup> /s)	2.4E-06	2.4E-06	2.4E-06	2.4E-06	2.4E-06
Stanton number, $St$	1.1	2.4	3.7	5.6	10.5
Biot number, $Bi$	1.07	0.76	0.97	0.76	0.61

$$\varepsilon_p \frac{\partial C}{\partial t} + v_r \frac{\partial C}{\partial t} + 3(1 - \varepsilon_p) \frac{k_L}{r_p} (C - C^*) = 0, \quad (2)$$

$$\frac{\partial q}{\partial t} = D_s \left( \frac{\partial^2 q}{\partial r^2} + \frac{2}{r} \frac{\partial q}{\partial r} \right). \quad (3)$$

It would be shown later in this study from the AIC criterion analysis, Freundlich isotherm would be the most suitable model to describe the isothermal equilibrium between the diluted fluid mass and adsorbed mass in solid phase. The non-linear temperature-independent Freundlich isotherm equation couples the two partial differential equations through the adsorption term of the transport equation. With the non-linear adsorption isotherm embedded, it becomes highly challenging to find an analytical solution. Solutions to the set of PDEs along with the boundary and initial conditions were obtained using finite differences method as published in literature (Sperlich *et al.*, 2008). All calculations were performed using the software FAST 2.0 Beta (Fixed-bed Adsorption Simulation Tool) that was developed originally for water treatment applications.

## 2.4 Calculation of mass transfer coefficients

In order to estimate the dimensionless numbers, several model parameters need to be determined either through experiments or through empirical correlations. The column and adsorbent geometric parameters such as particle size, particle density ( $\rho_a$ ), particle porosity ( $\varepsilon_p$ ), superficial velocity, empty bed contact time, bed porosity ( $\varepsilon$ ), influent initial concentration ( $C_0$ ) were directly measured. Film diffusion coefficients,  $k_L$  and surface diffusion coefficients,  $D_s$  were estimated using the Gnielinski correlation which is a function of Reynolds and Schmidt numbers and Sonthheimer correlation, respectively (Sperlich *et al.*, 2008):

$$k_L = \frac{[1 + 1.5(1 - \varepsilon)]D}{d_p} [2 + 0.644\text{Re}^{1/2}\text{Sc}^{1/3}], \quad (4)$$

$$D_s = \frac{D\varepsilon_p C_0}{\tau_p \rho_a q_0} \times \text{SPDFR}. \quad (5)$$

In the above equations,  $D$  represents molecular diffusivity and is calculated as:

$$D = \frac{13.26 \times 10^{-05}}{\eta^{1.14} V_b^{0.589}}, \quad (6)$$

where,  $\eta$  is kinematic viscosity,  $V_b$  is normal molar volume,  $\tau_p$  is tortuosity (set to 1),  $q_0$  is equilibrium loading, and SPDFR is the surface to pore diffusion flux ratio.

## 2.5 HSDM model validation

HSDM can be satisfactorily used to predict breakthrough curves for different adsorption column sizes and flow conditions, without any experimental data *a priori*. However, in order to establish reliability and confidence over the chosen isotherm model and mass transfer correlations, HSDM predictions were first compared to lab-scale experimental data generated using different sized adsorption columns and flow rates with CAB adsorbent of 1 mm particle size. Five different adsorption column experiments were designed representing varying residence times. The bed porosity was maintained between 0.35 and 0.5 by adjusting the mass of adsorbent loaded into the column. Experiments were run using lean MDEA with an initial concentration of 3250–3500 ppm and breakthrough data were recorded as a function of residence time. The corresponding Biot and Stanton numbers have also been shown in Table 2 along with other process conditions. The same feed and process conditions were provided as input to the HSDM model and simulations

were performed to predict the complete breakthrough curves. Instead of comparing  $C/C_0$  at certain points, HSDM simulation provides a way to compare the entire BTC which is significant in establishing similarities in flow pattern between scales.

## 2.6 Sensitivity analysis

To investigate the effect of these dimensionless numbers on breakthrough curves, Pérez-Foguet *et al.* developed a dimensionless analysis of HSDM (Pérez-Foguet *et al.*, 2013). The macroscale liquid phase mass transport equation and the intraparticle diffusion equation were transformed into a dimensionless form using dimensionless variables for the liquid and solid phase concentration, axial position and contact time. The derivation of the dimensionless model equations and the corresponding boundary and initial conditions could be found elsewhere (Sperlich *et al.*, 2008). The two characteristic partial differential equations of the HSDM were transformed into a system of two ordinary differential equations coupled with the macroscale transport-reaction PDE. Discretization was accomplished using a discontinuous Galerkin scheme and the overall system evolution was integrated with a time-marching scheme based on the forward Euler method. The overall system was successfully used to simulate the adsorption of different adsorbates on granular ferric hydroxide.

The detailed dimensionless analysis of HSDM presented by Pérez-Foguet *et al.* (2013) facilitates establishing limit behavior of the model to determine the values of Bi and St number (Pérez-Foguet *et al.*, 2013). The influence of dimensionless numbers, including Bi, St, Ed,  $D_g$  and  $n$  on the breakthrough curves was thoroughly assessed using the dimensionless HSDM. Excerpts from this work have been presented in Section 3.3 and the results have been directly applied to determine the working range of Bi and St numbers.

Design parameters from this technique were compared with direct scale-up and kinetic approaches. Details of these two conventional techniques, including key equations have been summarized in the Supplementary Section.

## 3. Results and discussion

### 3.1 Equilibrium studies

Different isotherm models were fitted to batch equilibrium data and the model parameters were determined by non-linear regression. Equilibrium isotherms for TOA adsorption on CAB adsorbents have been presented in the Supplementary Section, see Figure S1. Figure 3 shows the comparison of simulated data from various models with batch equilibrium data obtained by varying adsorbent mass at 23 °C and Table 3 shows the regressed model parameters and the corresponding AIC values for different isotherm models. It can be noticed that the Freundlich model exhibited the least AIC value indicating the best fit with experimental data. Hence, Freundlich model was incorporated into the HSDM model to describe the equilibrium behavior between the solute present in the liquid and solid phases.

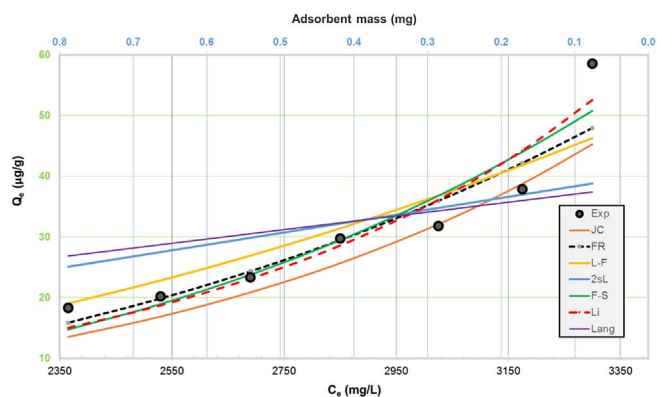


**Fig. 3.** Comparison of batch equilibrium data with various isotherm models (legend details: Exp – experimental, JC – Jovononic, FR – Freundlich, L-F – Langmuir-Freundlich, 2sL – 2 step-Langmuir, F-S – Fritz-Schlunder, Lang – Langmuir).

### 3.2 HSDM model validation

Figure 4 shows a comparison plot of normalized concentration against adsorption time between lab-scale experimental data and HSDM predictions for different residence times. An inset has been provided in order to better visualize the dynamics at early adsorption times. As shown in Figure 4, HSDM is able to capture the overall process dynamics described by the “S” shaped curve for all the HRT’s considered. Also, the general trend in BTC time-shift with varying HRTs was predicted reasonably well by the HSDM. On comparison of simulated BTCs with experimental data in Figure 4, some discrepancies are evident, especially for the case of HRT = 137 min. Many different factors influence the shape of the BTCs, primarily the values of mass transfer coefficients employed in the HSDM. The sensitivity of these coefficients has been analyzed *via* two dimensionless parameters, namely Bi and St numbers. As outlined in Section 3.3 and in the range of Bi values considered, St remains a significant parameter in determining BTC dynamics. However, in order to minimize the discrepancies between experimental data and simulation, the coefficients should be determined accurately from controlled batch experiments rather than from empirical correlations. Other known possible factors that influence BTC dynamics include HSDM assumptions concerning negligible pore diffusion and unaccounted experimental factors like backpressure and influent pumping issues encountered during column experiments. Nevertheless, as shown in this study, HSDM could be employed for the rapid design of the adsorption column where the application of other techniques is severely challenged by the inherent dependency on experimental data.

### 3.3 Sensitivity analysis

Sensitivity analysis on the dimensionless numbers provides knowledge on the variation of column breakthrough behavior in different scales. Breakthrough curves were predicted for ranges of St and Bi numbers to understand the mass transfer behavior at different process conditions. The

**Table 3.** Summary of isotherm model equations and parameters.

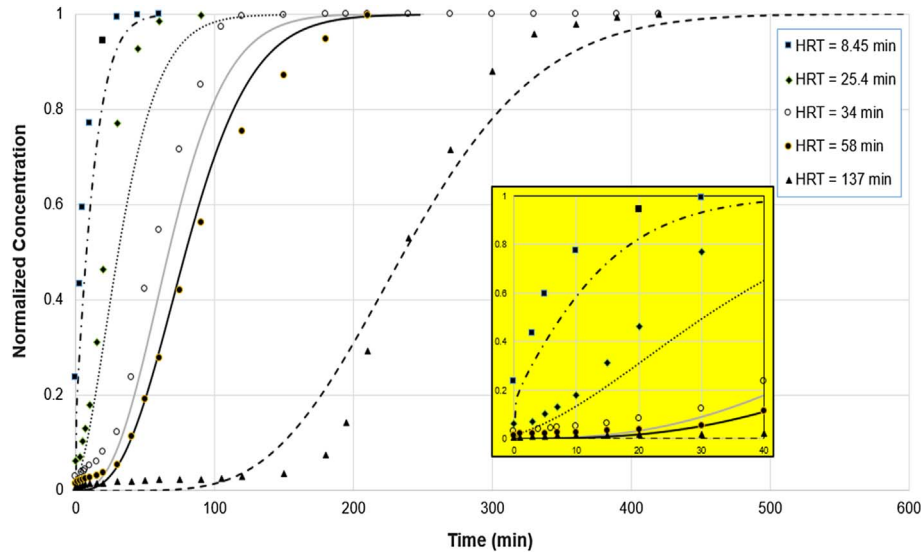
Isotherm model	Equation	Model fitting parameters	Values	AIC
Langmuir	$q = \frac{q_m b C}{1 + b C}$	$q_m, b$	$q_m = 37.8 \text{ mg/g}$ $b = 0.027 \text{ L/g}$	55.2
Langmuir-Freundlich	$q = \frac{q_m b C^n}{1 + b C^n}$	$q_m b, n$	$q_m = 837 \text{ mg/g}$ $b = 1.06\text{E-}11 \text{ (L/mg)}^n$ $n = 2.77$	37.9
Jovanovic	$q = q_m [1 - \exp(-a_j C)] [\exp(b_j C)]$	$q_m, a_j, b_j$	$q_m = 82.5 \text{ mg/g}$ $a_j = 7.6\text{E-}06 \text{ L/mg}$ $b_j = 0.0009 \text{ L/mg}$	38.6
Fritz-Schlunder	$q = \frac{\alpha_1 C^{\beta_1}}{1 + \alpha_2 C^{\beta_2}}$	$\alpha_1, \alpha_2, \beta_1, \beta_2$	$\alpha_1 = 2\text{E-}07 \text{ (mg}^{(1-\beta_1)} \text{ L}^{\beta_1})/\text{g}$ $\alpha_2 = 43625.5 \text{ (L/mg)}^{\beta_2}$ $\beta_1 = 3.71$ $\beta_2 = 0.0001$	48.8
Freundlich	$q = k_F C^n$	$k_F, n$	$k_F = 0.0015 \text{ ((mg/g)(L/mg)}^n)$ $n = 0.8$	28.7
Li	$q = K_L \ln \left[ 1 + (b_0 C)^{1M} \right]$ $\frac{1}{M} = \frac{1 + \ln [1 + b_L C]}{M_0}$	$K_L, b_0, M_0, b_L$	$k_L = 6.513 \text{ (mmol/g)}$ $b_0 = 0.014$ $M_0 = 0.332$ $b_L = 0.015 \text{ (L/mmol)}$	77.1
Two-step Langmuir	$q = \frac{a_1 b_1 C}{1 + b_1 C} + \frac{a_2 b_2 [(C - c_2) + \text{abs}(C - c_2)]}{2 + b_2 [(C - c_2) + \text{abs}(C - c_2)]}$	$a_1, b_1, a_2, b_2, c_2$	$a_1 = 43.56$ $b_1 = 6.1\text{E-}06$ $a_2 = 2.86\text{E+}04 \text{ (meq/g)}$ $b_2 = 5.04\text{E-}07 \text{ (L/meq)}$ $c_2 = 667.5 \text{ (meq/L)}$	100.5

analysis is based on a comparison of normalized concentration  $C/C_0$  versus dimensionless time  $T$ , defined as the ratio of operation time to ideal (stoichiometric) breakthrough time.

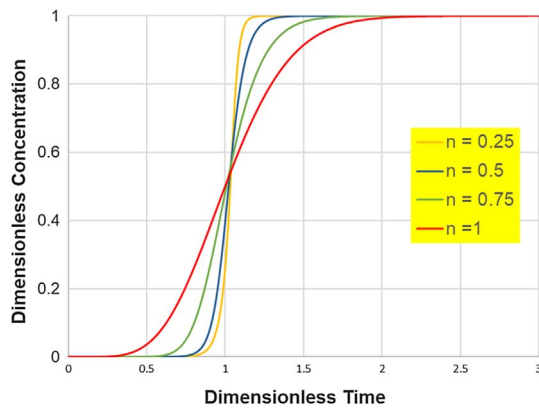
The values of dimensionless parameters of the lab-scale experiment used for HSDM validation study are presented in Table 2. Since solute distribution parameter ( $D_g$ ) and Freundlich exponent ( $n$ ) were determined from batch experiments in this study, they were treated as constants and not included in the sensitivity analysis. Further, since  $\text{Ed} = \text{St}/\text{Bi}$ , the influence of  $\text{Ed}$  is dependent on the individual values of  $\text{Bi}$  and  $\text{St}$  numbers. Detailed results on the dimensionless analysis could be found elsewhere (Pérez-Foguet *et al.*, 2013) and only key findings have been discussed in this section. It was shown by Pérez-Foguet *et al.* that BTC shapes and limit behaviors for both linear and nonlinear cases ( $n \leq 1$ ) are similar with minor differences in the sharpness of the wave-front. This was also verified in this study by performing a dimensionless analysis on “ $n$ ” varying from 0.25 to 1 (equivalent to an initial concentration of 7.5–3250 mg/L) while keeping  $\text{Bi}$  and  $\text{St}$  constant at 0.9 and 10, respectively. As it could be seen from

Figure 5, the effect of  $n$  is not so significant on the BTC dynamics and thus extrapolation of Freundlich isotherm towards zero adsorbate concentration may be assumed to impart negligible discrepancies in the HSDM predictions. Hence for all subsequent sensitivity and scale-up studies, the value of  $n$  was held constant at the regressed value of 0.8.

A representative plot illustrating the effect of  $\text{St}$  at low and high  $\text{Bi}$  numbers, see Figures 6a and 6b, was reproduced and assessed using the dimensionless HSDM system. Variation of  $\text{St}$  at fixed  $\text{Bi}$  would be attained by varying the flow velocity of the solvent flowing through the packed bed column. Breakthrough curves shown in both the plots were generated by varying Stanton numbers between 0 and  $10^4$  for fixed  $\text{Bi}$  values of 0.9 and 100 while other dimensionless parameters,  $D_g$  and  $n$  were held constant. At low  $\text{Bi}$  number, film diffusion dominates and thus acts as the controlling mechanism. Since differences between the results obtained at smaller pairs of  $\text{Bi}$  number were negligible (Pérez-Foguet *et al.*, 2013), only  $\text{Bi} = 0.9$  and  $\text{Bi} = 100$  were considered for the analysis. Also, since limit behavior was



**Fig. 4.** Validation of HSDM with lab-scale BTC data (lines represent simulation and marker represents lab data, inset depicts the goodness of fit at lower times).



**Fig. 5.** Effect of Freundlich exponent on breakthrough curve dynamics

found at these values for  $Bi$ , the predicted breakthrough curves are strongly dependent on  $St$  number as evidenced in Figure 6. At  $Bi$  number close to 1 and  $St > 10$ , refer Figure 6a, Mass Transfer Zone (MTZ) pattern is fully established as indicated by the sinusoidal BTC shaped curves. This regime ( $St > 10$ ) could be thought of instantaneous adsorption regime where film transfer dominates advection. However, at  $St < 10$ , the MTZ is still developing and shows a varying trend, indicating relatively slower adsorption and at  $St = 0$ , the condition changes to no adsorption. Also, since  $Bi$  number is small and close to 1, the BTCs are purely dependent on  $St$  number within the range from 0 to 10. However, at higher  $Bi$  number and thus higher  $Ed$ , see Figure 6b, when intraparticle diffusion is rate controlling, BTC shows a varying trend till the value of  $St$  is around 1000. The sensitiveness of breakthrough curves at low Stanton number ( $St < 10$ ) was evident in the lab-scale column experiments reported in

previous sections. As a comparison, Test 2 and Test 4 were run at varying Stanton numbers (Test 2:  $St = 2.4$ , Test 4:  $St = 5.6$ ) and at constant Biot number of 0.76. It can be noticed from Figure 4 that the dynamics of the two breakthrough curves are different with significant difference in breakthrough times.

Thus, columns of different sizes would exhibit similar mass transfer behavior or similar controlling mechanism if  $Bi$  was chosen close to 1 and  $St \geq 10$ . This analysis provided a working range of influent flow rates and loading rates or superficial velocity that could serve as a guideline while designing adsorption columns of larger scales.

HSDM assumes that solid phase mass transfer occurs only by surface diffusion and hence tortuosity and SPDFR are not considered significant. The sensitivity of intraparticle diffusion coefficient ( $D_s$ ) was tested on the BTC characteristics in a wide range from  $10^{-11}$  to  $10^{-9}$   $m^2/s$ , see Figure 7. The effect of  $D_s$  on the BTC dynamics could be better understood through analysis of the dimensionless Biot number. Since  $Bi$  and  $D_s$  are inversely proportional, increasing  $D_s$  by two orders of magnitude from  $10^{-11}$  to  $10^{-9}$  would proportionally decrease  $Bi$  that would eventually lead to faster adsorption characterized by sharp wavefront. Figure 8 illustrates the dimensionless BTC for different Biot numbers and a fixed  $St$  of 10. This implies a case of constant film transfer rate and flow velocity but varying surface diffusion efficient. As it can be noticed from sharpness of the wavefront, adsorption rate increases with decreasing  $Bi$  or increasing  $D_s$ . However, the effect of  $Bi$  on BTC shape beyond  $Bi = 0.1$  (or  $10^{-1}$ ) is not significant and practically remains unchanged, thereby setting the limits for surface diffusion coefficient.

By performing a sensitivity analysis on the Freundlich exponent, the impact of extrapolation of model parameters could be analyzed. BTC shapes and limit behaviors for both linear and nonlinear cases ( $n \leq 1$ ) are similar with minor differences in the sharpness of the wave-front

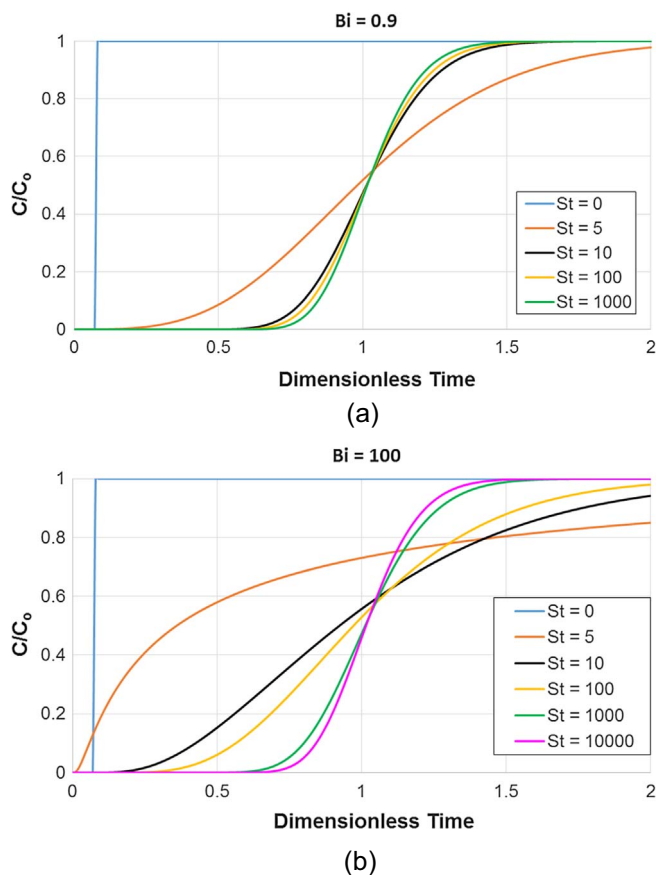


Fig. 6. Effect of Stanton number on the breakthrough curves at (a) Bi = 0.9, (b) Bi = 100.

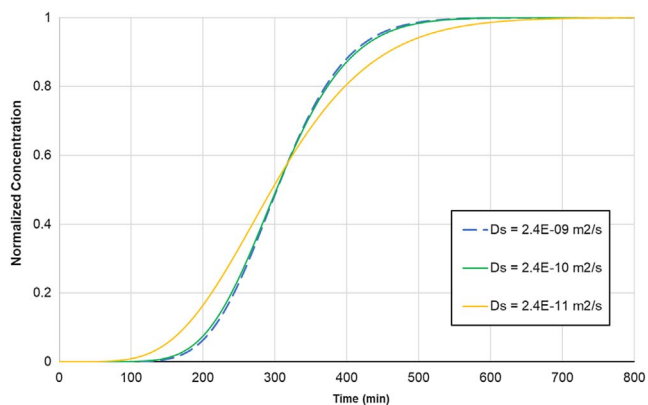


Fig. 7. Effect of surface diffusion coefficient on BTC dynamics.

(Pérez-Foguet *et al.*, 2013). This was also verified in this study by performing a dimensionless analysis on “*n*” varying from 0.25 to 1 (equivalent to an initial concentration of 7.5 to 3250 mg/L) while keeping Bi and St constant at 0.8 and 10, respectively. As it could be seen from Figure 9, the effect of Freundlich exponent is not so significant on the BTC dynamics and thus extrapolation of Freundlich isotherm towards zero adsorbate concentration can be assumed to have negligible influence on the HSDM predictions. Hence

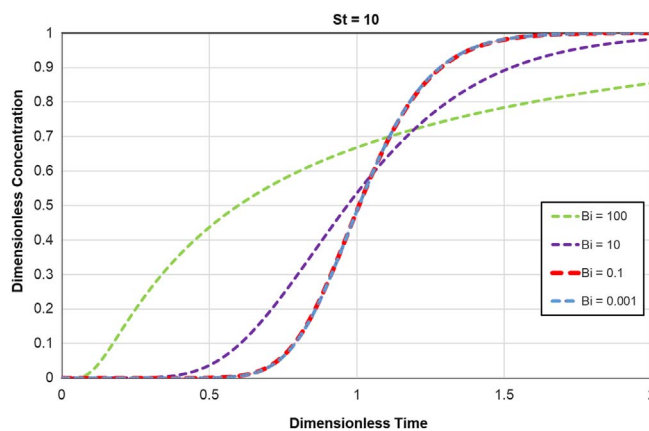


Fig. 8. Effect of Biot number on Dimensionless BTC dynamics.

for all sensitivity and scale-up studies, the value of *n* was held constant at the regressed value of 0.8.

### 3.4 Design scale assessment

From sensitivity analysis, the range of Bi and St numbers that would exhibit similar mass transfer phenomena for TOA adsorption were determined. Based on these results, a pilot-scale adsorption column was designed using the critical design parameter rules recommended by Inglezakis and Pouloupoulos, as shown in Table 1. For all subsequent analysis, lab-scale test column Case 3, shown in Tables 2 and 4, was chosen as the representative lab-scale design and compared with the pilot-scale design parameters.

Figure 10 illustrates the complete breakthrough curves predicted for different scales using the validated HSDM. The scales from the lab to pilot differ in residence time; however, the critical design parameters remain the same. For a lab-scale column with a residence time of 34 min, the estimated breakthrough time was *ca.* 26 min that is in good agreement with the experimentally determined value of 28.5 min. Similarly, pilot-scale unit with a residence time of 205 min resulted in relatively higher breakthrough times of *ca.* 330 min.

As expected, breakthrough time to attain a normalized effluent concentration of 0.1 increases with increasing residence time. It should be noted that mass transfer coefficients were calculated by empirical correlations from the literature because they are not scalable from batch-scale studies to pilot-scale studies due to differences in flow pattern in the reactor. The accuracy of HSDM predictions depends strongly on the appropriateness of these correlations and the estimated equilibrium parameters from batch studies.

Additionally, the column design was carried out using the conventional packed-bed scale-up procedure and simplified kinetic models (detailed in the Supplementary Section) and compared with the HSDM design parameters. It is worth noting that both the scale-up and the kinetic approach depends entirely on the breakthrough data generated using test column, either laboratory or pilot plant. In the scale-up approach using the Length of Unused Bed (LUB) model, the loading rate and the unused bed length

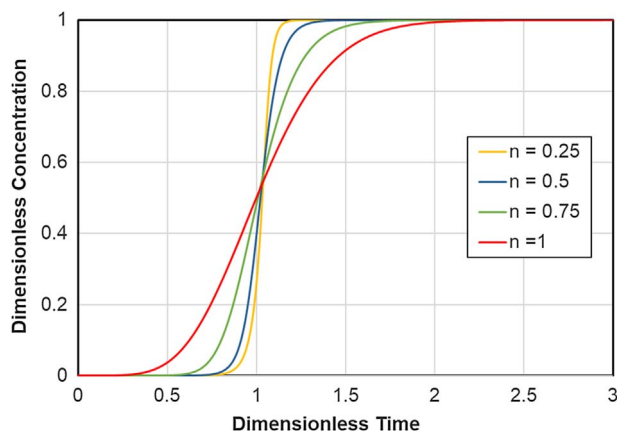


**Fig. 9.** Effect of Freundlich exponent on breakthrough curve dynamics.

**Table 4.** Summary of lab-scale and pilot-scale adsorption column design parameters.

Parameter	Lab test column	Pilot column	Scale-up factor
Adsorber bed height, $L$ (cm)	23	150	6.5
Bed diameter, $D$ (cm)	4.6	30	6.5
Adsorbent particle diameter, $d_p$ (mm)	1	1	–
$L/D$	5	5	–
$L/d_p$	230	1500	–
$D/d_p$	46	300	–
Equivalent bed mass (kg)	0.26	70	270
MDEA flow rate (mL/min)	4.3	185	43
Empty bed contact time (min)	89	573	6.5
Residence time (min)	34	205	6.5
Superficial velocity (cm/min)	0.26	0.26	1
Stanton number, $St$	3.7	24	–
Biot number, $Bi$	0.97	0.91	–

for both the lab-scale and pilot-scale units had to be maintained constant to obtain similar mass transfer characteristics. In this study, the lab-scale test column of 4.3 cm diameter and 23 cm height was used with a filtration or loading rate of  $0.256 \text{ cm}^3/\text{min cm}^2$  and an EBCT of 96 min. The length of unused bed corresponding to the fraction of bed unused was calculated as 13.1 cm. As per the LUB model, this length should remain the same in scale-up, and thus the length of unused bed in pilot-plant design was taken as 13.1 cm and the corresponding breakthrough time was estimated as 345 min.

The kinetic approach was based on the simplified Bohart and Adams model that employed a kinetic rate

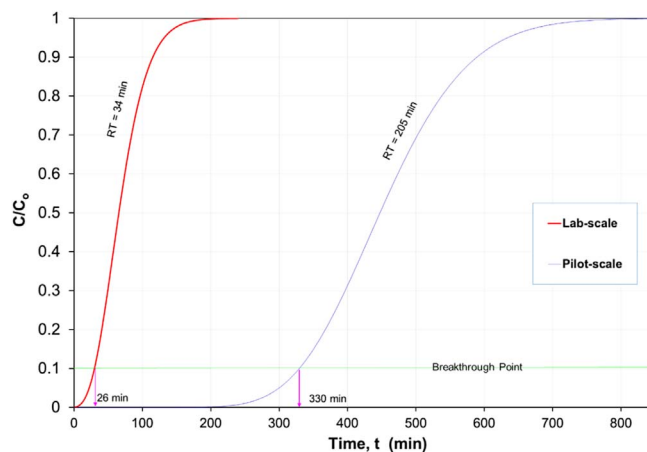


**Fig. 10.** Comparison of BTC curves between different scales as predicted by HSDM.

**Table 5.** Comparison of pilot-scale design parameters between various techniques.

Design parameter	HSDM	Scale-up	Kinetic
Column diameter (cm)	30	30	30
Bed height (cm)	150	160	160.2
Flow rate (cc/min)	185	185	185
Adsorbent mass (kg)	70.6	70.7	79.7
Breakthrough time (min)	330	370	330
Maximum solid phase loading (mg/g)	3.85	N/A	2.8
Breakthrough volume (L)	61.5	68.5	61.5

equation to determine the reaction constant and maximum solid phase loading. However, this approach necessitates a breakthrough volume or time to be specified in the design equation. A breakthrough time of 335 min (taken from HSDM) was used to calculate other design parameters including the mass of adsorbent required and breakthrough volume. Table 5 shows a comparison of various design parameters calculated from different techniques. It can be noted that all three techniques yield similar results for the design of a pilot-scale adsorber, however with different complexities. HSDM could be used to design adsorption column of various scales with minimal input about equilibrium data and mass transfer coefficients. However, the other two techniques, scale-up, and kinetic approaches are dependent on the accuracy of the supplied breakthrough data.

## 4 Conclusion

The objective of the present work was to utilize the predictive homogeneous surface diffusion model for designing a fixed-bed adsorber to remove TOA present in lean MDEA solution using CAB adsorbent. As part of the design technique, various isotherm models were fitted to batch equilib-

rium data, and based on Akaike Information Criterion (AIC), it was found that the equilibrium isotherms were best described by the Freundlich equation. Subsequently, Freundlich isotherm parameters and appropriate mass transfer correlations for film and surface diffusivities were incorporated into the HSDM equation matrix. Numerical solution to the simultaneous transport-reaction equations and non-linear Freundlich equation was executed through commercial software. Simulation results were compared with lab-scale experimental data collected at lower residence times (<140 min), and it was evident that HSDM could predict breakthrough curves with reasonable accuracy. Dimensionless HSDM equations were employed to describe the limit behavior of the model based on dimensionless numbers, Bi and St. Sensitivity analysis on the two parameters established the operating range for the design units as  $Bi \sim 1$  and  $St > 10$ . Further, in order to preserve the flow pattern during scale-up process, key column parameters and similitude rules from literature were reviewed and integrated into the column design. Based on the design guidelines, 30 cm by 150 cm fixed-bed adsorber with a continuous throughput of 11.1 L/h was considered suitable. HSDM predicted a 330 min column operating time with an equivalent lean amine treatment capacity of 60 L based on a 10% breakthrough limit for the designed column. Accuracy of the HSDM based design technique was evaluated by comparing with conventional scale-up and kinetic approaches and was found to be in good agreement. Results demonstrated the rapid, ease-of-use and accuracy of the HSDM technique for the design of fixed-bed adsorption columns for complex systems.

## Supplementary materials

The supplementary material of this article is available at <https://ogst.ifpenergiesnouvelles.fr/10.2516/ogst/2020073/olm>. Details of these two conventional techniques (scale-up approach, kinetic approach), including key equations have been summarized in the supplementary section.

*Fig. S1.* Plot of  $\ln((C_0/C_t) - 1)$  vs. time.

*Table S1.* Kinetic parameters obtained by linear regression

*Fig. S2.* Adsorption equilibrium curve,  $q_e$  vs  $C_e$  for the adsorptive removal of TOA using CAB composites.

*Supplementary References.*

*Acknowledgments.* The authors would like to acknowledge the support provided by the *Gas Research Center (GRC)* at *Khalifa University* under research grant GRC11006.

## References

Chowdhury Z.Z., Hamid S.B., Zain S.M. (2015) Evaluating design parameters for breakthrough curve analysis and kinetics of fixed bed columns for Cu(II) cations using lignocellulosic wastes, *BioResources* **10**, 1, 732–749.  
Crittenden B., Thomas W.J. (1998) *Adsorption technology and design*, Butterworth-Heinemann, Woburn, MA, USA.

Crittenden J.C., Berrigan J.K., Hand D.W. (1986a) Design of rapid small-scale adsorption tests for a constant diffusivity, *J. Water Pollut. Control Fed.* **58**, 4, 312–319.  
Crittenden J.C., Hand D.W., Arora H., Lykins B.W. (1987) Design considerations for GAC treatment of organic chemicals, *J. Am. Water Works Ass.* **79**, 1, 74–82.  
Crittenden J.C., Hutzler N.J., Geyer D.G., Oravitz J.L., Friedman G. (1986b) Transport of organic compounds with saturated groundwater flow: Model development and parameter sensitivity, *Water Resour. Res.* **22**, 3, 271–284.  
Crittenden J.C., Reddy P.S., Arora H., Trynoski J. (1991) Predicting GAC performance with Rapid Small-Scale Column Tests, *J. Am. Water Works Ass.* **83**, 1, 77–87.  
Cummings A.L., Smith G.D., Nelson D.K. (2007) Advances in amine reclaiming: Why there is no excuse for operating a dirty amine system, in: *Laurance Reid Gas Conditioning Conference*, Dickinson TX, USA, pp. 227–244.  
Dávila-Jiménez M.M., Elizalde-González M.P., García-Díaz E., González-Perea M., Guevara-Villa M.R.G. (2014) Using akaike information criterion to select the optimal isotherm equation for adsorption from solution, *Adsorpt. Sci. Technol.* **32**, 7, 605–622.  
Edathil A.A., Pal P., Banat F. (2018) Alginate clay hybrid composite adsorbents for the reclamation of industrial lean methyldiethanolamine solutions, *Appl. Clay Sci.* **156**, 213–223.  
Edathil A.A., Pal P., Kannan P., Banat F. (2020) Total organic acid adsorption using alginate/clay hybrid composite for industrial lean amine reclamation using fixed-bed: Parametric study coupled with foaming, *Int. J. Greenh. Gas. Con.* **94**, 102907.  
Hand D.W., Crittenden J.C., Arora H., Miller J.M., Lykins B.W. (1989) Designing fixed-bed adsorbents to remove mixtures of organics, *J. Am. Water Works Ass.* **81**, 1, 67–77.  
Hand D.W., Crittenden J.C., Thacker W.E. (1983) User-oriented batch reactor solutions to the homogeneous surface diffusion model, *J. Environ. Eng.* **109**, 1, 82–101.  
Hand D.W., Crittenden J.C., Thacker W.E. (1984) Simplified models for design of fixed-bed adsorption systems, *J. Environ. Eng.* **110**, 2, 440–456.  
Hudaya T., Rachmat V. (2019) Activated carbon fixed-bed adsorber design for treating chromium hexavalent wastewater, *Makara J. Technol.* **22**, 3, 135–141.  
Inglezakis V.J., Pouloupoulos S.G. (2006) *Adsorption, Ion Exchange and Catalysis*, Elsevier, Amsterdam, The Netherlands.  
Keewan M., Banat F., Pal P., Zain J., Alhseinat E. (2018) Foaming of industrial lean methyldiethanolamine solution in the presence of hydrocarbon and fatty acid based corrosion inhibitors, *Oil Gas Sci. Technol. - Rev. IFP Energies nouvelles* **73**, 76, 1–7.  
Lee M.C., Crittenden J.C., Snoeyink V.L., Ari M. (1983) Design of carbon beds to remove humic substances, *J. Environ. Eng.* **109**, 3, 631–645.  
Mehassouel A., Derriche R., Bouallou C. (2018) Kinetics study and simulation of CO<sub>2</sub> absorption into mixed aqueous solutions of methyldiethanolamine and hexylamine, *Oil Gas Sci. Technol. - Rev. IFP Energies nouvelles* **73**, 19, 1–10.  
Pal P., AbuKashabeh A., Al-Asheh S., Banat F. (2015) Role of aqueous methyldiethanolamine (MDEA) as solvent in natural gas sweetening unit and process contaminants with probable reaction pathway, *J. Nat. Gas Sci. Eng.* **24**, 124–131.  
Pal P., Banat F., AlShoaibi A. (2013) Adsorptive removal of heat stable salt anions from industrial lean amine solvent using anion exchange resins from gas sweetening unit, *J. Nat. Gas Sci. Eng.* **15**, 14–21.

- Pal P., Edathil A.A., Banat F. (2019) Calcium alginate gel and hard beads for the removal of total organic acid anions and heavy metal ions from industrial lean methyldiethanolamine solvent, *Polym. Bull.* **76**, 1, 103–118.
- Patel H. (2019) Fixed-bed column adsorption study: a comprehensive review, *Appl. Water Sci.* **9**, 45, 1–17.
- Pérez-Foguet A., Casoni E., Huerta A. (2013) Dimensionless analysis of HSDM and application to simulation of breakthrough curves of highly adsorbent porous media, *J. Environ. Eng.* **139**, 5, 667–676.
- Smith E.H. (1997) Wave front analysis for design of fixed-bed adsorbers, *Chem. Eng. Commun.* **159**, 1, 17–37.
- Sperlich A., Schimmelpfennig S., Baumgarten B., Genz A., Amy G., Worch E., Jekel M. (2008) Predicting anion breakthrough in Granular Ferric Hydroxide (GFH) adsorption filters, *Water Res.* **42**, 8–9, 2073–2082.
- Srivastava V.C., Prasad B., Mishra I.M., Mall I.D., Swamy M. M. (2008) Prediction of breakthrough curves for sorptive removal of phenol by bagasse fly ash packed bed, *Ind. Eng. Chem. Res.* **47**, 5, 1603–1613.
- Traegner U.K., Suidan M.T. (1989) Parameter evaluation for carbon adsorption, *J. Environ. Eng.* **115**, 1, 109–128.
- Verma N., Verma A. (2009) Amine system problems arising from heat stable salts and solutions to improve system performance, *Fuel Process. Technol.* **90**, 4, 483–489.
- Weiland R. (2008) Heat stable salts and amine unit performance, *Hydrocarbon World* **3**, 1, 30–33.
- Wolborska A. (1999) External film control of the fixed bed adsorption, *Chem. Eng. J.* **73**, 2, 85–92.
- Xu Z., Cai J., Pan B. (2013) Mathematically modeling fixed-bed adsorption in aqueous systems, *J. Zhejiang Univ. Sci. A* **14**, 3, 155–176.
- Younas O., Banat F. (2014) Parametric sensitivity analysis on a GASCO's acid gas removal plant using ProMax simulator, *J. Nat. Gas Sci. Eng.* **18**, 247–253.